International Journal of Mechanical Sciences 51 (2009) 443–452

Contents lists available at ScienceDirect

International Journal of Mechanical Sciences

journal homepage: www.elsevier.com/locate/ijmecsci

Modal characteristics of symmetrically laminated composite plates flexibly restrained at different locations

W.F. Hao, T.Y. Kam *

Mechanical Engineering Department, National Chiao Tung University, Hsin Chu 300, Taiwan, Republic of China

ARTICLE INFO

Article history:
Received 28 May 2008
Received in revised form
25 March 2009
Accepted 26 March 2009
Available online 9 April 2009

Keywords:
Composite plate
Free vibration
Modal analysis
Rayleigh–Ritz method
Structural analysis
Composite materials

ABSTRACT

A method for determining modal characteristics (natural frequencies and mode shapes) of symmetrically laminated composite plates restrained by elastic supports at different locations in the interior and on the edges of the plates is presented. The classical lamination theory together with an appropriate set of characteristic functions are used in the Rayleigh–Ritz method to formulate the eigenvalue problem for determining the modal characteristics of the flexibly supported laminated composite plates. Sweep-sine vibration testing of several laminated composite plates flexibly restrained at different locations on the plates is performed to measure their natural frequencies. The close agreement between the experimental and theoretical natural frequencies of the plates has verified the accuracy of the proposed method. The effects of elastic restraint locations on the modal characteristics of flexibly supported laminated composite plates with different lamination arrangements and aspect ratios are studied using the present method. The usefulness of the results obtained for predicting sound radiation behavior of flexibly supported laminated composite plates is discussed.

1. Introduction

Because of their many advantageous properties, composite materials are used to make structural parts in different industries. For instance, laminated composite plates are used to fabricate aircraft structures in the aerospace industry, vehicle parts in the automotive industry, and flat-panel speakers in the audio industry. In general, laminated composite plates used to fabricate these structures/parts are joined together via flexible connectors or restrained by other structural components, which act as flexible supports to the plates. For aircraft and vehicle structures, the determination of the actual dynamic behavior of the flexibly supported plates in the structures is an important task if unwanted vibrations or noise radiated from the structures are to be suppressed. For laminated composite flat-panel speakers, it is also important to determine the actual dynamic properties of the flexibly supported laminated composite sound radiating plates of the speakers if the generation of high-quality sound is desired. In general, the motion of a flexibly supported plate consists of two parts, namely vertical rigid body motion and flexural vibration. The vertical rigid body motion contributes mainly to the sound radiation of the plate in the low-frequency range while the flexural vibration contributes to that in the mid- to high-frequency range. In designing a flat-panel speaker, since sound quality in the audible frequency range depends on the motion of the sound radiating plate, the determination of accurate modal characteristics of such plates has become an important topic of research.

In the past several decades, many researchers have studied the free vibration of plate structures and proposed different techniques to determine their natural frequencies [1–10]. For instance, Ashton [1] used the Ritz method to study the natural frequencies and modes of free anisotropic square plates. In his study, the effects of anisotropy on the natural frequencies and mode shapes were investigated. Leissa [2] attempted to present comprehensive and accurate analytical results for the free vibration of rectangular plates. Hung et al. [3] presented an eigenvalue formulation for the free vibration analysis of symmetrically laminated rectangular plates with elastic edge restraints. In their study, the first 10 natural frequencies were determined. Ding [4] used a set of static beam functions in the Ritz method to study the free vibration of thin isotropic rectangular plates with elastic edge restraints. In general, most of the papers on free vibration analysis of plates have focused on the determination of their modal characteristics for regular boundary conditions, e.g., simply supported edges or flexible supports around the whole periphery. It is not uncommon that for specific applications, plates may be flexibly supported at particular locations inside or along their boundaries. Regarding the free vibration of such plates, it seems that few, if any, investigations have been reported. If deeper understanding of the modal characteristics of plates with different kinds of elastic supports is to be achieved, research investigation must be initiated.

* Corresponding author.
E-mail address: tykam@mail.nctu.edu.tw (T.Y. Kam).

0020-7403/$ - see front matter © 2009 Elsevier Ltd. All rights reserved.
doi:10.1016/j.ijmecsci.2009.03.013

In this paper, the Rayleigh–Ritz method is used for the free vibration analysis of laminated composite plates supported by elastic restraints at different locations in the interior and along the edges of the plates. Experiments are performed to measure the natural frequencies of several laminated composite plates supported by elastic restraints at different locations in order to verify the accuracy of the proposed method. A number of examples are presented to quantify the effects of the positions of the restraints on the modal characteristics of laminated composite plates with different lamination arrangements and aspect ratios.

2. Plate vibration analysis

A thin rectangular symmetrically laminated composite plate of length a_o, width b_o, and constant thickness h composed of n layer groups is supported by elastic strips of width b_S and depth h_S at portions of the periphery of the plate and excited by a circular moving coil-type shaker in the interior of the plate as shown in Fig. 1(a). Herein, the rigid frame is used to position the edge elastic strips and shaker. As shown in Fig. 1(b), the damper together with the voice coil of the shaker works as an interior circular elastic restraint of radius r_c to support the plate in which the fiber angle of the kth layer group is θ_k. In the plate vibration analysis, the length and width of the plate are a and b, respectively, the edge elastic restraints are modeled as distributed rotational and translational springs, and the interior elastic restraint is modeled as a ring-type spring system of radius r_c composed of distributed translational springs as shown in Fig. 2(a). Herein, the x- and y-coordinates of the x–y–z Cartesian coordinate system lie in the mid-plane of the plate. Fig. 2(b) shows the locations of the elastic restraints in the x–y plane. For instance, the center of the interior ring-type spring system is located at (x_c, y_c), y_{p-1} and y_p are the coordinates of the end points of the pth edge elastic support on the edge at $x = 0$, and x_{q-1} and x_q are the coordinates of the end points of the qth edge elastic support on the edge at $y = 0$. In the present model, the edge springs are located at one half of the widths of the edge elastic restraints and the length and width of the plate are $a = a_o - b_S$ and $b = b_o - b_S$, respectively. For the laminated plate, if the deflection of the plate is $w(x, y)$, based on the classical lamination theory [11], the strain energy of the plate, U_p, can be expressed as

$$U_P = \frac{1}{2}\int_0^a \int_0^b \left[D_{11}\left(\frac{\partial^2 w}{\partial x^2}\right)^2 + 2D_{12}\left(\frac{\partial^2 w}{\partial x^2}\right)\left(\frac{\partial^2 w}{\partial y^2}\right) + D_{22}\left(\frac{\partial^2 w}{\partial y^2}\right)^2 + 4D_{66}\left(\frac{\partial^2 w}{\partial x\,\partial y}\right)^2 + 4D_{16}\left(\frac{\partial^2 w}{\partial x^2}\right)\left(\frac{\partial^2 w}{\partial x\,\partial y}\right) + 4D_{26}\left(\frac{\partial^2 w}{\partial y^2}\right)\left(\frac{\partial^2 w}{\partial x\,\partial y}\right)\right] dy\,dx \quad (1)$$

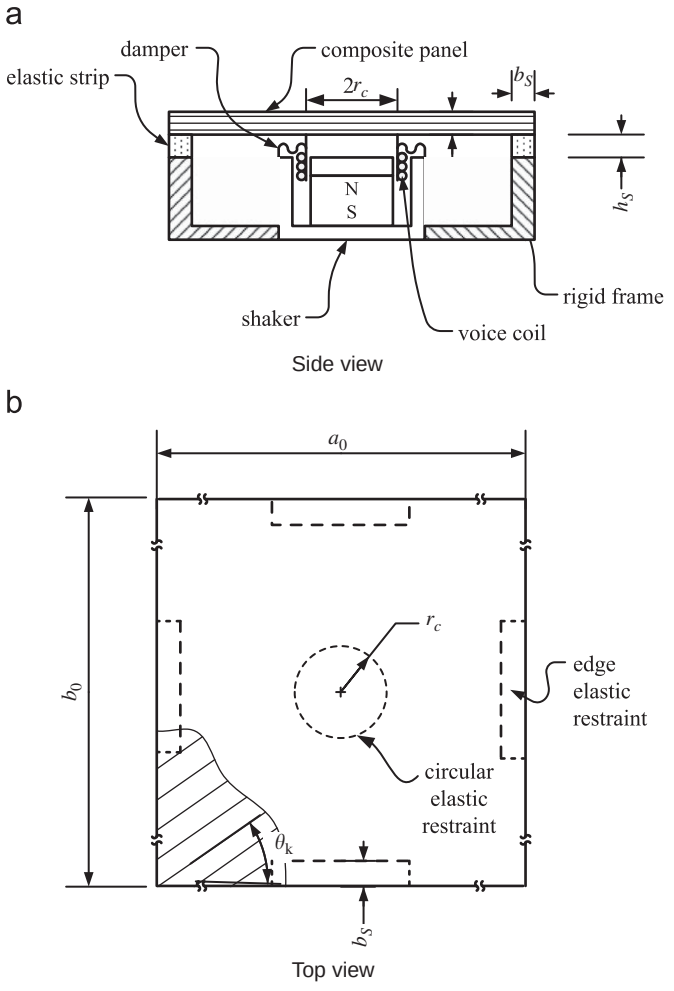

Fig. 1. Flexibly supported laminated composite plate excited by a moving coil-type shaker.

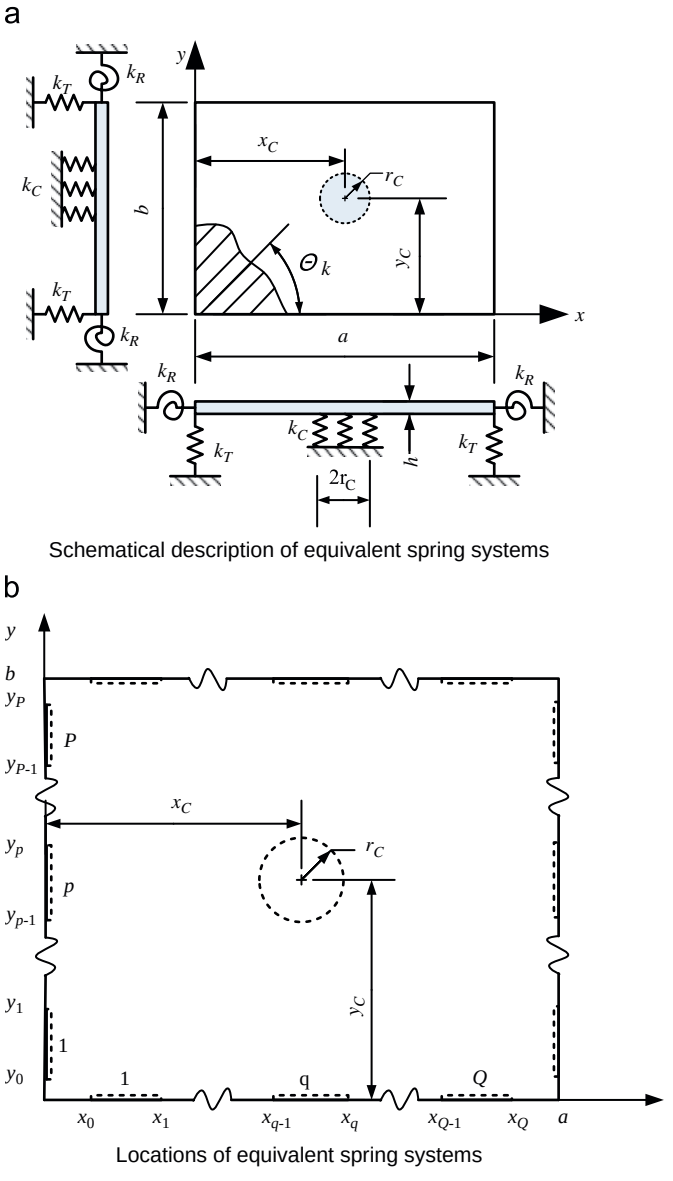

Fig. 2. Mathematical model of elastically supported plate.

In the above equation, the bending stiffness coefficients D_{ij} are given as

$$D_{ij} = \frac{1}{3}\sum_{k=1}^{n} (\bar{Q}_{ij})_k (z_k^3 - z_{k-1}^3); \quad i,j = 1,2,6 \tag{2}$$

where the transformed stiffness coefficients $(\bar{Q}_{ij})_k$ of the kth layer depend on the material properties and fiber orientation θ_k of the layer. For $\theta_k = 0$, the transformed stiffness coefficients can be written as

$$\bar{Q}_{11} = \frac{E_1}{1 - v_{12}v_{21}}; \quad \bar{Q}_{12} = \frac{v_{12}E_2}{1 - v_{12}v_{21}};$$
$$\bar{Q}_{22} = \frac{E_2}{1 - v_{12}v_{21}}; \quad \bar{Q}_{66} = G_{12} \tag{3}$$

where E_1 and E_2 are Young's moduli parallel and transverse to the fiber directions, respectively; v_{ij} is the Poisson ratio for transverse strain in the jth direction when stressed in the ith direction, and G_{12} is shear modulus. The maximum kinetic energy of the plate is expressed as

$$T = \frac{\rho h \omega^2}{2} \int_0^a \int_0^b w^2 dy\, dx \tag{4}$$

where ω is circular vibration frequency and ρ is mass per unit area of the plate. For the plate restrained by an interior elastic support and several symmetrically located elastic restraints on the edges, additional strain energy is stored in the equivalent springs. The strain energy associated with the elastic restraints, U_S, is

$$U_S = \left\{ \sum_{p=1}^{P} \left[\int_{y_{p-1}}^{y_p} w^2\, dy \right]_{x=0} + \sum_{q=1}^{Q} \left[\int_{x_{q-1}}^{x_q} w^2\, dx \right]_{y=0} \right\} k_T + \left\{ \sum_{p=1}^{P} \left[\int_{y_{p-1}}^{y_p} \left(\frac{\partial w}{\partial x} \right)^2 dy \right]_{x=0} + \sum_{q=1}^{Q} \left[\int_{x_{q-1}}^{x_q} \left(\frac{\partial w}{\partial x} \right)^2 dx \right]_{y=0} \right\} k_R + \oint_I \frac{k_C}{2} w^2\, dl \tag{5}$$

where P and Q are number of edge elastic restraints on the edges at $x = 0$ and $y = 0$, respectively; k_T and k_R are spring constant intensities (spring constants per unit length) for, respectively, edge translation and rotation springs; k_c is interior translational spring constant intensity; $\oint_I$ is line integral around the periphery of the ring-type support, and dl is a differential arc length of the circumference of the ring-type support. In view of Eqs. (1) and (5), the total strain energy, U, of the flexibly supported plate can be expressed as

$$U = U_P + U_S \tag{6}$$

In the Rayleigh–Ritz method, the deflected shape of the plate undergoing free vibration is approximated in the following dimensionless form:

$$w(\xi,\eta) = \sum_{i=1}^{I}\sum_{j=1}^{J} C_{ij}\phi_i(\xi)\psi_j(\eta) \tag{7}$$

where C_{ij} are the unknown coefficients; ϕ_i, ψ_j are characteristic functions of the same form; ξ, η are nondimensional coordinates with $\xi = -1+2x/a$ and $\eta = -1+2y/b$. It is noted that the origin of the ξ–η coordinate system is located at the plate center. The adopted characteristic functions ϕ_i are chosen from the following two sets of functions, i.e., for $i \leqslant 4$,

$$\phi_1(\xi) = \tfrac{1}{2} - \tfrac{3}{4}\xi + \tfrac{1}{4}\xi^3$$
$$\phi_2(\xi) = \tfrac{1}{8} - \tfrac{1}{8}\xi - \tfrac{1}{8}\xi^2 + \tfrac{1}{8}\xi^3$$
$$\phi_3(\xi) = \tfrac{1}{2} + \tfrac{3}{4}\xi - \tfrac{1}{4}\xi^3$$
$$\phi_4(\xi) = -\tfrac{1}{8} - \tfrac{1}{8}\xi + \tfrac{1}{8}\xi^2 + \tfrac{1}{8}\xi^3 \tag{8}$$

and for $i > 4$,

$$\phi_i(\xi) = \sin(A_i\xi + A_i)\sin\left(\frac{\pi}{2}\xi + \frac{\pi}{2}\right), \quad i = 5,6,\ldots \tag{9}$$

where $A_i = \pi/2(i-4)$. It is noted that the cubic displacement functions of Eq. (8) are beam element shape functions. Similarly, the characteristic functions ψ_j can be obtained by replacing ϕ_i and ξ in Eqs. (8) and (9) by ψ_j and η, respectively. The rigid body motion of the flexibly supported plate has been taken into consideration in Eq. (8). It is noted that the displacement field obtained using the adopted characteristic functions may only satisfy the kinematic boundary conditions of the plate. The extremization of the functional $I = U - T$ with respect to C_{ij} leads to the following eigenvalue problem:

$$[\underline{\mathbf{K}} - \omega^2 \underline{\mathbf{M}}]\underline{\mathbf{C}} = \underline{\mathbf{0}} \tag{10}$$

where $\underline{\mathbf{K}}$ and $\underline{\mathbf{M}}$ are stiffness and mass matrices of the flexibly supported plate, respectively; $\underline{\mathbf{C}}$ is the vector of unknown coefficients C_{ij}. The stiffness matrix $\underline{\mathbf{K}}$ can be written as the sum of the following two parts:

$$\underline{\mathbf{K}} = \underline{\mathbf{K}}^P + \underline{\mathbf{K}}^S \tag{11}$$

where $\underline{\mathbf{K}}^P$ and $\underline{\mathbf{K}}^S$ are the plate bending and elastic restraint stiffnesses, respectively. The elements in $\underline{\mathbf{M}}$, $\underline{\mathbf{K}}^P$, and $\underline{\mathbf{K}}^S$ are expressed, respectively, as

$$M_{ijmn} = \frac{a^2\rho h}{8\alpha} I_{im}^{00} J_{jn}^{00} \tag{12}$$

$$K_{ijmn}^P = \frac{2}{a^2\alpha}\left[D_{11} I_{im}^{22} J_{jn}^{00} + \alpha^2 D_{12}\left(I_{im}^{20} J_{jn}^{02} + I_{im}^{02} J_{jn}^{20} \right) + \alpha^4 D_{22} I_{im}^{00} J_{jn}^{22} + 4\alpha^4 D_{66} I_{im}^{11} J_{jn}^{11} + 2\alpha D_{16}\left(I_{im}^{21} J_{jn}^{01} + I_{im}^{01} J_{jn}^{21} \right) + 2\alpha^3 D_{26}\left(I_{im}^{10} J_{jn}^{12} + I_{im}^{12} J_{jn}^{10} \right) \right] \tag{13}$$

and

$$K_{ijmn}^S = \frac{a}{4\alpha} k_T \sum_{p=1}^{P}\left[F_{jn}^p \phi_i(-1)\phi_m(-1) + F_{jn}^p \phi_i(1)\phi_m(1) \right] + \frac{a}{4} k_T \sum_{q=1}^{Q}\left[E_{im}^q \psi_j(-1)\psi_n(-1) + E_{im}^q \psi_j(1)\psi_n(1) \right] + \frac{1}{a\alpha} k_R \sum_{p=1}^{P}\left[F_{jn}^p \phi_i'(-1)\phi_m'(-1) + F_{jn}^p \phi_i'(1)\phi_m'(1) \right] + \frac{\alpha^2}{a} k_R \sum_{q=1}^{Q}\left[E_{im}^q \psi_j'(-1)\psi_n'(-1) + E_{im}^q \psi_j'(1)\psi_n'(1) \right] + \frac{a r_C k_C}{4\alpha^2} G_{mnij} \tag{14}$$

with

$$I_{im}^{rs} = \int_{-1}^{1} \frac{d^r \phi_i(\xi)}{d\xi^r} \frac{d^s \phi_m(\xi)}{d\xi^s}\, d\xi,$$
$$J_{jn}^{rs} = \int_{-1}^{1} \frac{d^r \psi_j(\eta)}{d\eta^r} \frac{d^s \psi_n(\eta)}{d\eta^s}\, d\eta \tag{15}$$

$$E_{im}^p = \int_{\xi_{p-1}}^{\xi_p} \phi_i(\xi)\phi_m(\xi) d\xi, \quad F_{jn}^q = \int_{\eta_{q-1}}^{\eta_q} \psi_j(\eta)\psi_n(\eta) d\eta \tag{16}$$

$$G_{mnij} = \int_0^{2\pi} \phi_m\left(\frac{2r_C}{a}\cos\theta \right)\phi_n\left(\frac{2r_C}{a}\cos\theta \right) \times \varphi_i\left(\frac{2r_C}{b}\sin\theta \right)\varphi_j\left(\frac{2r_C}{b}\sin\theta \right) d\theta \tag{17}$$

where $\alpha = a/b$; $r, s = 1, 2$; the integration is performed around the circumference of the interior support. The modal characteristics of the plate can then be determined from Eq. (10) using the characteristic functions given in Eqs. (8) and (9).

3. Experimental investigation

The natural frequencies of rectangular T300/PR313 graphite/epoxy $[90^\circ/0^\circ]_S$ and $[30^\circ/-30^\circ]_S$ laminated composite plates partially supported on the edges by a number of strip-type foam/adhesive pads and in the interior by a circular shaker were determined experimentally. The foam/adhesive pad was composed of a foam core and two thin adhesive films on, respectively, the top and bottom surfaces of the core. The dimensions ($a_o \times b_o$) of the laminated composite plates were either 100 mm × 100 mm or 70 mm × 140 mm while the thicknesses of the $[90^\circ/0^\circ]_S$ and $[30^\circ/-30^\circ]_S$ plates were 0.6 and 0.62 mm, respectively. The material constants of the plates were determined in accordance with ASTM standards D3039 and 3518 [12]. In each test, three specimens were used to determine the average values of the material constants, which are given as

$$E_1 = 148\,\text{GPa}(0.723\%), \quad E_2 = 9\,\text{GPa}(1.189\%)$$
$$G_{12} = 7\,\text{GPa}(3.158\%), \quad v_{12} = 0.3(0.189\%) \tag{18}$$

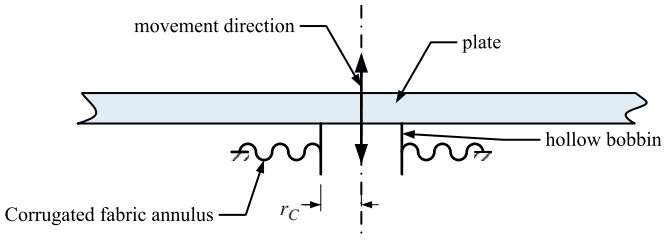

Fig. 3. Interior ring-type elastic support.

where the values in the parentheses denote coefficients of variation. In this study, the translational and rotational spring constant intensities of the strip-type pads with cross-sectional dimensions of width b_S and depth h_S determined via the strength of materials approach are expressed, respectively, as [13]

$$k_T = \frac{E_S b_S}{h_S} \quad \text{and} \quad k_R = \frac{E_S b_S^3}{12 h_S} \tag{19}$$

The dimensions of the flexibly supported plate used in the vibration analysis then become $a = a_o - b_S$ and $b = b_o - b_S$. Herein, for simplicity, the foam/adhesive pad was treated as an isotropic and homogeneous solid. The experimental equivalent elastic constant, E_S, of the foam/adhesive pad was 3.75×10^4 Pa. The spring constant intensities of the pad-type support with cross-sectional dimensions $b_S = 2$ mm and $h_S = 1$ mm were calculated as $k_T = 7.5 \times 10^4\,\text{N/m}^2$ and $k_R = 0.025$ N. The shaker in Fig. 1 is used to vibrate the plate so that the natural frequencies can be determined. As shown in Fig. 1, the top end and lower part of the voice coil of the shaker are bonded to the bottom surface of the plate and a corrugated damper, respectively. The coil and damper work as a ring-type elastic support restraining the vertical displacement of the plate as shown in Fig. 3. The spring constant intensity of the interior ring-type elastic support was determined from the measured load–displacement curve of the shaker. For the interior support of radius $r_c = 12.5$ mm, $k_C = 1.29 \times 10^4\,\text{N/m}^2$. The centers of the interior ring-type supports were at (50, 50 mm) or (25, 25 mm) on the square plate and (70, 35 mm) or (35, 35 mm) on the rectangular plate. The edge support conditions of the plates are shown in Fig. 4.

The experimental setup for the plate vibration study is shown in Fig. 5. In the vibration testing of the flexibly supported plate,

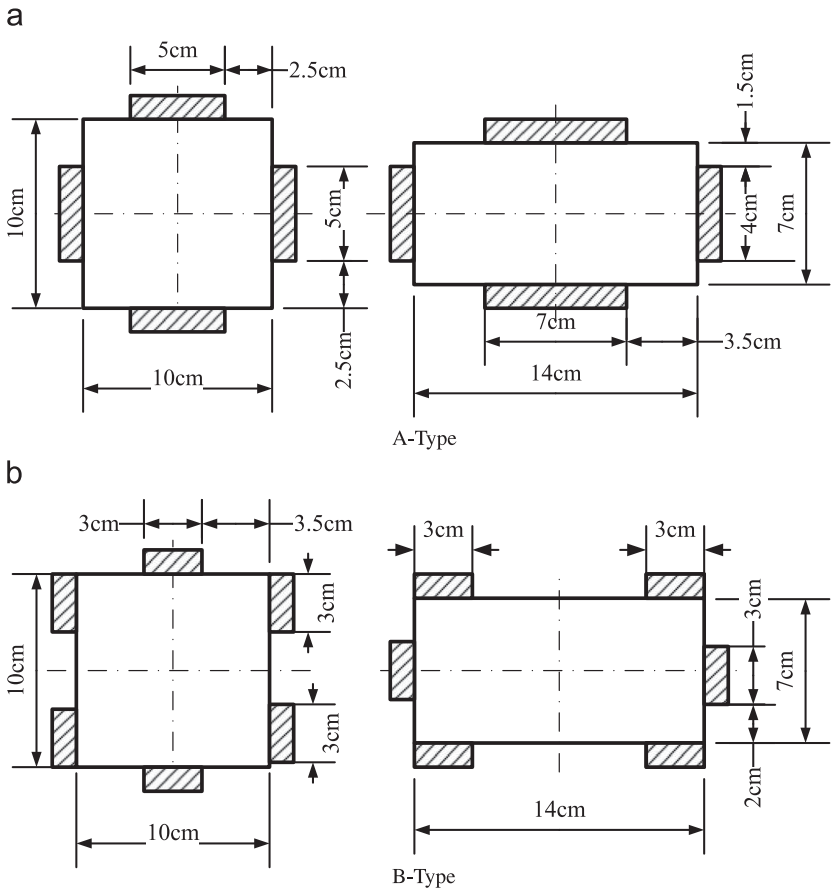

Fig. 4. Edge elastic restraints of laminated composite plates with different aspect ratios.

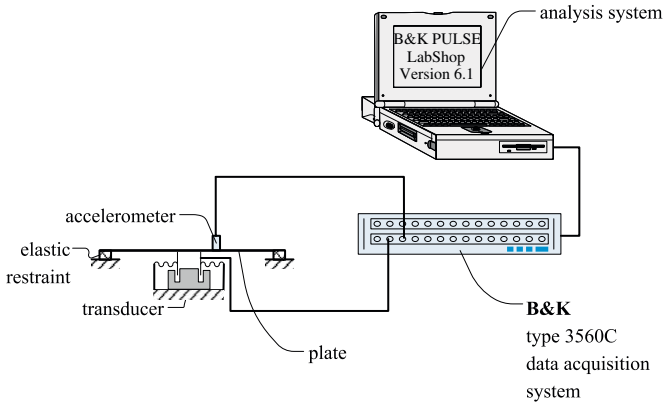

Fig. 5. Experimental setup for vibration testing.

the B&K 3650C-type data acquisition system was used to provide sweeping harmonic sine function signals in a specific frequency range to the electro-magnetic shaker for exciting the plate. The plate response signals picked up by the accelerometer attached to the surface of the plate were analyzed using the FFT analyzer of the data acquisition system to construct the frequency response spectrum of the plate. The accelerometer was placed at 3 different locations on the plate to measure the plate responses for identifying the mode numbers associated with the natural frequencies. One easy way of identifying the mode numbers was to locate the nodal lines on the plate. In determining the natural frequencies of the plate, it was assumed that the accelerometer mass of 0.4 g was so small that its effects on the vibration behavior of the plate were negligible. Furthermore, the modal damping ratios of values less than 3% for the first 12 modes were small enough to be neglected in the determination of the natural frequencies. The natural frequencies of the flexibly supported plate were then extracted from the frequency response spectra generated by the data acquisition system.

4. Results and discussions

A convergence study of the proposed analysis method was performed first. A series of convergence tests has shown that for flexibly restrained laminated composite plates with different support conditions, the use of 12×12 terms in Eq. (8) can obtain the first 35 natural frequencies with sufficient accuracy. For instance, the percentage difference between the natural frequencies of the 35th mode obtained using 12×12 and 13×13 terms is 0.07%. The ability of the present Rayleigh–Ritz method to predict accurate modal characteristics of laminated composite plates supported by edge springs has been validated by comparison with results reported in the literature [3,14]. The ability of the present method to predict the experimentally determined natural frequencies of flexibly supported graphite/epoxy $[90^\circ/0^\circ]_S$ and $[30^\circ/-30^\circ]_S$ plates was then studied. The first 12 theoretical natural frequencies and mode shapes of the square and rectangular plates are listed, respectively, in Tables 1 and 2 where they are compared with the experimental results. It is noted that since the diameter of the voice coil was small compared to the size of the plate, the modes with nodal lines passing through the center of the shaker, i.e., the point of excitation, could not be detected during the vibration tests. Therefore, the natural frequencies associated with these modes could not be measured and are not listed in Tables 1 and 2. The percentage differences between the theoretical and experimental natural frequencies of the square plates listed in Table 1 are less than or equal to 3.4% while those of the rectangular plates are less than or equal to 7.86%. The percentage differences between the theoretical and experimental natural frequencies may be due to variations in material properties, over-simplified modeling of the elastic supports and/or measurement inaccuracies. But for practical applications, especially for the design of flat-panel speakers, such percentage differences are acceptable.

Next the effects of different boundary conditions and aspect ratios on the modal characteristics of the graphite/epoxy $[90^\circ/0^\circ]_S$ and $[30^\circ/-30^\circ]_S$ plates are studied. It has been shown that the effects on the $[90^\circ/0^\circ]_S$ and $[30^\circ/-30^\circ]_S$ plates are similar. For instance, Table 3 shows the mode shapes associated with the first 12 natural frequencies of the square $[90^\circ/0^\circ]_S$ plate with free or flexibly restrained boundary conditions. It is noted that for the free boundary conditions, the spring constant intensities of the edge and interior elastic supports are set as zero, while for the flexibly restrained boundary conditions, the spring constant intensities determined in the experimental investigation are adopted in the vibration analysis. As is well known, the flexible supports can magnify the natural frequencies and change the mode shapes of the free square $[90^\circ/0^\circ]_S$ plate. In particular, the natural frequencies of the flexibly supported plates with an interior elastic restraint are higher than those of the flexibly supported plates without an interior elastic restraint. For a given edge support condition, the percentage differences between the natural frequencies of the plates with an interior elastic support and those of the plates without an interior elastic support, however, diminish as the mode number increases. For instance, considering the first normalized natural frequency of square plates comprising A-type edge elastic supports, the percentage differences between the plates with and without an interior elastic support are less than or equal to 22.1% and 23.0%, respectively, for the $[90^\circ/0^\circ]_S$ and $[30^\circ/-30^\circ]_S$ plates, while for the twelfth natural frequencies, the corresponding percentage differences are less than or equal to 0.46% and 0.27%. To further illustrate the effects of elastic supports on the natural frequencies of the $[90^\circ/0^\circ]_S$ plate, Fig. 6 shows the normalized natural frequency distributions of the free plate and the plate with B-type edge support and an interior support. It is noted that for mode numbers higher than 12 or normalized natural frequencies higher than 5, the differences between the normalized natural frequencies of the plates with different support conditions are negligible and this implies that elastic supports have insignificant effects on the normalized natural frequencies of higher modes. Regarding the mode shapes of the plates under consideration, it seems that the elastic restraints have more effect on the lower than on the higher modes. In particular, the mode shapes of the plates with or without elastic supports tend to become the same for mode numbers higher than or equal to the twelfth mode. It is noted that the details of the plate modal characteristics are important in the design of flat-panel speakers. Considering a flat-panel speaker excited by a relatively small moving coil-type shaker, the location of the interior elastic support is the same as that of the voice coil of the shaker. Regarding the plates under consideration, the modes with nodal lines passing through the center of the interior elastic support will not be activated by the shaker and thus have no contribution to sound radiation from the panels. For instance, among the 12 modes of the centrally supported square $[90^\circ/0^\circ]_S$ plate with B-type edge elastic support, only the symmetric bending modes such as the first, fifth, seventh, and tenth modes of the plate can be activated by the shaker for sound radiation. On the contrary, for the same plate but with an off-center elastic support, both symmetric and asymmetric modes such as modes 2, 6, 9, and 11 will be activated for sound radiation. It is further noted that the locations of the edge elastic supports may have significant effects on the mode shapes of the plates. For instance, the shapes of modes 2, 4, 7, 8, 10, and 11 of the centrally

Table 1
Theoretical and experimental natural frequencies of square flexibly supported composite plates.

Layup (mass density)	Edge support	Interior support	Natural frequency (Hz)												
			Mode No.	1	2	3	4	5	6	7	8	9	10	11	12
$[90^\circ/0^\circ]_S$ (1269 Kg/m^3)	A-type	Center	Experiment	236.5	–	–	–	442.2	–	–	707.1	–	–	967.0	–
			Present method	240.52	241.51	257.42	260.37	431.11	505.45	688.47	700.74	843.90	899.40	969.61	1348.78
				(1.71)[a]	–	–	–	(−2.62)	–	–	(−0.90)	–	–	(0.28)	–
		Off-center	Experiment	204.3	250.5	–	317.9	417.3	511.7	–	695.0	852.3	912.3	943.8	–
			Present method	206.05	245.85	257.36	322.79	417.88	509.07	688.07	702.76	847.12	907.13	956.06	1345.01
				(0.87)	(−1.86)	–	(1.55)	(0.15)	(−0.51)	–	(1.12)	(−0.61)	(−0.56)	(1.29)	–
	B-type	Center	Experiment	225.3	–	–	–	463.9	–	677.8	–	–	972.6	–	–
			Present method	226.26	268.60	290.06	357.61	460.94	617.24	671.12	690.19	841.14	972.55	974.48	1335.44
				(0.43)	–	–	–	(−0.65)	–	(−0.99)	–	–	(−0.)	–	–
		Off-center	Experiment	195.0	269.9	311.8	387.3	439.7	599.8	–	–	841.7	–	955.2	–
			Present method	192.54	276.30	314.19	388.72	453.75	620.22	663.59	695.30	839.77	963.93	979.53	1333.03
				(−1.26)	(2.37)	(0.77)	(0.37)	(3.20)	(3.40)	–	–	(0.23)	–	(2.55)	–
$[30^\circ/-30^\circ]_S$ (1315 Kg/m^3)	A-type	Center	Experiment	234.0	–	–	–	417.3	–	606.6	–	–	881.8	1081.4	1281.9
			Present method	237.35	246.89	271.40	299.02	423.46	509.09	597.67	710.45	805.76	868.94	1082.06	1272.10
				(1.41)	–	–	–	(1.49)	–	(−1.46)	–	–	(−1.46)	(0.06)	(−0.76)
		Off-center	Experiment	204.3	268.1	287.0	317.9	419.6		608.6	719.0	796.2	852.3	1083.5	1292.9
			Present method	205.96	267.36	291.22	321.59	419.84	506.09	600.56	715.64	807.65	862.36	1082.21	1273.34
				(0.83)	(−0.29)	(1.46)	(1.18)	(0.07)	–	(−1.31)	(−0.47)	(1.43)	(1.18)	(−0.12)	(−0.02)
	B-type	Center	Experiment	219.3	–	–	366.9	408.9	–	647.9	–	–	872.7	1083.8	1275.0
			Present method	216.89	267.46	295.08	368.06	410.28	550.86	648.39	672.36	830.84	866.81	1071.35	1265.46
				(−1.10)	–	–	(0.32)	(0.34)	–	(0.08)	–	–	(−0.67)	(−1.15)	(−0.75)
		Off-center	Experiment	181.4	–	329.2	–	420.1	550.7	647.9	684.0	–	872.7	1083.8	1275.1
			Present method	179.84	265.17	328.35	379.80	420.49	551.71	640.22	680.66	830.57	864.81	1071.10	1265.60
				(−0.56)	–	(−0.26)	–	(0.09)	(0.18)	(−1.19)	(−0.49)	–	(−0.91)	(−1.18)	(−0.75)

[a] The value in the parentheses denotes the percentage difference between the experimental and theoretical natural frequencies, i.e., [(experimental value−theoretical value)/experimental value] × 100%.

Table 2
Theoretical and experimental natural frequencies of rectangular flexibly supported composite plates.

Layup (mass density)	Edge support	Interior support	Natural frequency (Hz)											
			Mode No.	1	2	3	4	5	6	7	8	9	10	11	12
$[90^\circ/0^\circ]_S$ (1287 Kg/m^3)	A-type	Center	Experiment	–	240.8	–	–	373.6	–	–	–	864.4	–	1341.4	–
			Present method	233.15	245.37	258.17	265.02	379.62	520.32	525.15	684.45	818.65	988.59	1253.10	1254.14
				–	(1.90)[a]	–	–	(1.61)	–	–	–	(−5.29)	–	(−6.58)	–
		Off-center	Experiment	–	–	–	285.3	–	–	535.3	–	864.5	–	–	1354.9
			Present method	223.56	260.12	270.28	289.08	348.10	519.32	527.10	686.51	814.97	987.43	1252.39	1256.56
				–	–	–	(1.32)	–	–	(−1.53)	–	(−5.73)	–	–	(−7.26)
	B-type	Center	Experiment	198.8	–	–	383.1	–	–	–	–	804.7	–	1306.9	–
			Present method	196.59	218.76	264.80	387.45	408.86	514.72	530.78	668.83	808.68	981.50	1241.99	1247.89
				(−1.11)	–	–	(1.14)	–	–	–	–	(0.49)	–	(−4.97)	–
		Off-center	Experiment	143.2	–	299.9	388.9	–	524.7	–	–	847.4	–	1341.4	–
			Present method	140.70	209.39	300.26	390.00	413.75	517.62	530.35	669.56	807.57	981.46	1235.95	1249.75
				(−1.75)	–	(0.23)	(0.28)	–	(−1.35)	–	–	(−4.73)	–	(−7.86)	–
$[30^\circ/-30^\circ]_S$ (1337 Kg/m^3)	A-type	Center	Experiment	238.4	–	–	321.6	447.2	–	621.8	–	–	890.7	1238.4	–
			Present method	244.36	245.19	301.34	317.80	441.80	538.31	607.47	720.88	854.28	858.34	1154.69	1271.30
				(2.50)	–	–	(−1.18)	(−1.21)	–	(−2.30)	–	–	(−3.63)	(−6.76)	–
		Off-center	Experiment	217.9	276.9	–	321.7	434.0	568.3	640.7	744.2	–	917.8	1201.9	–
			Present method	217.68	283.72	303.03	319.78	422.10	539.52	614.32	722.51	853.26	859.65	1155.62	1265.77
				(−0.10)	–	–	(−0.60)	(−2.74)	(−5.06)	(−4.12)	(−2.91)	–	(−6.34)	(−3.85)	–
	B-type	Center	Experiment	205.2	–	–	381.2	447.2	–	666.8	–	881.8	–	1189.9	––
			Present method	206.34	249.68	304.80	377.26	439.20	566.59	651.64	692.30	837.50	890.51	1130.60	1261.14
				(0.56)	–	–	(−1.03)	(−1.79)	–	(−2.27)	–	(−5.02)	–	(−4.98)	–
		Off-center	Experiment	166.4	–	321.7	385.0	447.2	585.6	660.2	–	–	945.7	1204.8	–
			Present method	166.05	254.08	323.81	389.49	441.29	568.08	640.63	692.36	836.17	897.94	1131.46	1256.34
				(−0.21)	–	(0.66)	(1.17)	(−1.32)	(−2.99)	(−2.96)	–	–	(−5.05)	(−6.09)	–

[a] The value in the parentheses denotes the percentage difference between the experimental and theoretical natural frequencies, ie, [(experimental value−theoretical value)/experimental value] × 100%.

Table 3
Modal characteristics of a square $[90^\circ/0^\circ]_S$ composite plate with different boundary conditions.

Edge Support	Interior Support	Modal characteristics												
		Mode No.	1	2	3	4	5	6	7	8	9	10	11	12
Free	no	Frequency (Hz)	0	0	0	138.99	263.56	386.15	584.69	646.18	728.00	838.42	857.68	1265.88
		Mode shape												
A-type	no	Frequency	187.36	241.35	256.12	256.19	410.54	501.88	683.04	697.40	841.52	899.00	954.84	1342.55
		Mode shape												
	center	Frequency	240.52	241.51	257.42	260.37	431.11	505.45	688.47	700.74	843.90	899.40	969.61	1348.78
		Mode shape												
	off-center	Frequency	206.05	245.85	257.36	322.79	417.88	509.07	688.07	702.76	847.12	907.13	956.06	1345.01
		Mode shape												
B-type	No	Frequency	167.92	263.51	286.62	357.39	446.30	615.41	659.44	690.04	832.98	963.10	974.17	1330.86
		Mode shape												
	center	Frequency	226.26	268.60	290.06	357.61	460.94	617.24	671.12	690.19	841.14	972.55	974.48	1335.44
		Mode shape												
	off-center	Frequency	192.54	276.30	314.19	388.72	453.75	620.22	663.59	695.30	839.77	963.93	979.53	1333.03
		Mode shape												

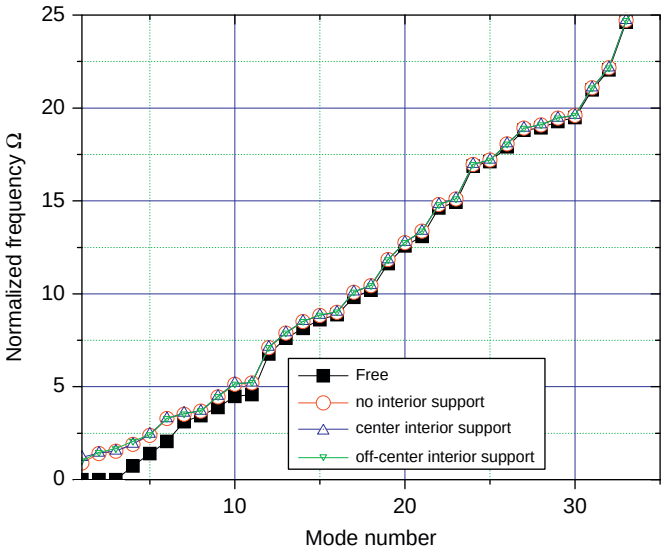

Fig. 6. Normalized natural frequency distribution of a square $[90^\circ/0^\circ]_S$ plate with different support conditions $\left(\Omega = \sqrt{\rho h \omega^2 a^4/D_0}\right)$.

restrained square $[90^\circ/0^\circ]_S$ plate with A-type edge support are completely different from those of the same plate but with B-type edge support. Nevertheless, as mentioned before, such effects start to diminish as the mode number reaches 12. As far as sound radiation is concerned, it is obvious that the support conditions have insignificant effects on the sound radiation behavior of the plate at frequencies higher than the twelfth natural frequency of the plate. Comparing the modal characteristics of the square $[90^\circ/0^\circ]_S$ plates with those of the square $[30^\circ/-30^\circ]_S$ plates, it is obvious that fiber angles have significant effects on the modal characteristics of the plates. The modal characteristics of the $[90^\circ/0^\circ]_S$ plates are totally different from those of the $[30^\circ/-30^\circ]_S$ plates even when the boundary conditions are the same. This implies that the sound radiation properties of the $[90^\circ/0^\circ]_S$ and $[30^\circ/-30^\circ]_S$ plates will be quite different even though they have the same support conditions. To study the effects of aspect ratio on the modal characteristics of the plates, Table 4 shows the mode shapes associated with the first 12 natural frequencies of the rectangular (aspect ratio = 2) $[90^\circ/0^\circ]_S$ plate with free or flexibly restrained boundary conditions. Like the square plates, the existence of the flexible supports can increase the natural frequencies and change the mode shapes of the free rectangular $[90^\circ/0^\circ]_S$ and $[30^\circ/-30^\circ]_S$ plates. For a given edge support condition, it is also noted that the percentage differences between the natural frequencies of the rectangular plates with an interior elastic support and those of the plates without an interior elastic support diminish as the mode number increases. For instance, for the rectangular $[90^\circ/0^\circ]_S$ and $[30^\circ/-30^\circ]_S$ plates with A-type edge elastic supports, the percentage differences between the first natural frequencies of the plates with a center support and those without a center support are less than or equal to 6.54% and 20.1%, respectively, while those of the twelfth natural frequencies for the plates with and without a center support are less than or equal to 0.40% and 0.56%, respectively. Regarding the mode shapes of the rectangular plates, just like the square plates, the elastic restraints of rectangular plates also have more significant effects on the shapes of lower modes than on those of higher modes. If the rectangular plate is also used as a flat-panel speaker, the modes with nodal lines passing through the center of the interior elastic support will not produce sound radiation. For instance, among the 12 modes under consideration, only the symmetric bending modes such as the 2, 5, 9, and 11

Table 4
Modal characteristics of a rectangular $[90^\circ/0^\circ]_S$ composite plate with different boundary conditions.

Edge Support	Interior Support	Modal characteristics												
		Mode No.	1	2	3	4	5	6	7	8	9	10	11	12
Free	no	Frequency (Hz)	0.	0.	0.	134.48	138.45	314.68	370.77	566.30	726.94	920.53	1193.33	1199.03
		Mode shape												
A-type	no	Frequency	217.90	229.35	258.09	264.66	342.92	514.55	518.19	683.93	806.82	985.91	1248.98	1251.50
		Mode shape												
	center	Frequency	233.15	245.37	258.17	265.02	379.62	520.32	525.15	684.45	818.65	988.59	1253.10	1254.14
		Mode shape												
	off-center	Frequency	223.56	260.12	270.28	289.08	348.10	519.32	527.10	686.51	814.97	987.43	1252.39	1256.56
		Mode shape												
B-type	No	Frequency	102.60	203.75	258.88	377.47	408.45	510.55	529.34	668.42	799.28	979.44	1231.43	1243.33
		Mode shape												
	center	Frequency	196.59	218.76	264.80	387.45	408.86	514.72	530.78	668.83	808.68	981.50	1241.99	1247.89
		Mode shape												
	off-center	Frequency	140.70	209.39	300.26	390.00	413.75	517.62	530.35	669.56	807.57	981.46	1235.95	1249.75
		Mode shape												

modes of the centrally restrained rectangular $[90^\circ/0^\circ]_S$ plate with A-type elastic support can be excited by the shaker and produce sound radiation. On the other hand, for the same plate with an off-center elastic support, both symmetric and asymmetric modes such as modes 4, 7, 9, and 12 will be excited for sound radiation as long as the nodal lines do not pass through the center of the off-center support. It is also noted that the locations of the edge elastic supports on the rectangular plates may have significant effects on the mode shapes. For instance, the shapes of modes 1, 2, 3, 4, and 5 of the centrally restrained rectangular $[90^\circ/0^\circ]_S$ plate with A-type edge support are completely different from those of the same plate but with B-type edge support. Just like the square plates, such effects start to diminish as the mode number reaches 12. It is further noted that aspect ratio has significant effects on the modal characteristics of the $[30^\circ/-30^\circ]_S$ plates. Irrespective of mode number, the modal characteristics of the square plates are quite different from those of the rectangular plates even though the two types of plate have similar boundary conditions. This implies that the sound radiation properties of the two types of plates will be different even though they have same lamination arrangements and similar support conditions.

5. Conclusions

A method for free vibration analysis of laminated composite plates peripherally and interiorly restrained by elastic supports has been constructed via the Rayleigh–Ritz approach. The accuracy of the present method has been verified by the experimental results obtained from the sweep-sine harmonic vibration testing of several laminated composite plates peripherally supported by discrete elastic strip-type pads and interiorly by a circular elastic restraint. The present method has been used to study the effects of the parameters such as locations of edge and interior elastic restraints, fiber angle, and plate aspect ratio on the modal characteristics of flexibly supported laminated composite plates. It has been shown that all the parameters may have significant effects on the natural frequencies and mode shapes of the flexibly supported laminated composite plates. But the effects induced by the locations of elastic restraints on modal characteristics may diminish, starting from the twelfth mode of the plates considered in this paper. The uses of the composite plates and the information of their modal characteristics in the design of flat-panel speakers have been discussed. The lower modes that are active in sound radiation of the laminated composite plates have been identified. The support conditions have insignificant effects on the sound radiation of the plates at frequencies higher than the twelfth natural frequencies of the plates. The results obtained in this study should be useful for gaining better understanding of the sound radiation behavior of laminated composite flat-panel speakers.

Acknowledgement

This research work was supported by the Veteran General Hospital University System of Taiwan of the Republic of China under Grant no. VGHUST97-P4-14. Its support is gratefully appreciated.

References

[1] Ashton JE. Natural modes of free-free anisotropic plates. The Shock and Vibration Bulletin 1969;39:93–100.
[2] Leissa AW. The free vibration of rectangular plates. Journal of Sound and Vibration 1973;31:257–93.
[3] Hung KC, Lim MK, Liew KM. Boundary beam characteristics orthonormal polynomials in energy approach for vibration of symmetric laminates-II: Elastically restrained boundaries. Composite Structures 1993;26:185–209.
[4] Ding Z. Natural frequencies of rectangular plates using a set of static beam functions in Rayleigh–Ritz method. Journal of Sound and Vibration 1996; 189(1):81–7.
[5] Beslin O, Nicolas J. A hierarchical function set for predicting very high order plate bending modes with any boundary condition. Journal of Sound and Vibration 1997;202(5):633–55.
[6] Al-Obeid A, Copper JE. A Rayleigh–Ritz approach for the estimation of the dynamic properties of symmetric composite plates with general boundary conditions. Composites Science and Technology 1995;53:289–99.
[7] Liew KM, Hing KC, Lim KM. Vibration of Mindlin plates using boundary characteristic orthogonal polynomials. Journal of Sound and Vibration 1995;182(1):77–90.
[8] Lee CR, Kam TY, Sun SJ. Free vibration analysis and material constants identification of laminated composite sandwich plates. ASCE Journal of Engineering Mechanics 2007;133(8):874–86.
[9] Bardell NS. Free vibration analysis of a flat plate using the hierarchical finite element method. Journal of Sound and Vibration 1991;151(2):263–89.
[10] Chang TP, Wu MH. On the use of characteristic orthogonal polynomials in the free vibration analysis of rectangular anisotropic plates with mixed

boundaries and concentrated masses. Computers & Structures 1997;62(4): 699–713.
[11] Jones RM. Mechanics of Composite Material. New York: McGraw-Hill Inc.; 1975.
[12] ASTM. Standards and literature references for composite materials, 2nd ed. West Conshohocken, PA, 1990.
[13] Lee CR, Kam TY. Identification of mechanical properties of elastically restrained laminated composite plates using vibration data. Journal of Sound and Vibration 2006;295:999–1016.
[14] Ding Z. Natural frequencies of elastically restrained rectangular-plates using a set of static beam functions in the Rayleigh–Ritz method. Computers & Structures 1995;57(4):731–5.